arXiv:2212.06060v1 [eess.IV] 12 Dec 2022

On Finite Difference Jacobian Computation in Deformable Image Registration

Yihao Liu, Junyu Chen, Shuwen Wei, Aaron Carass, and Jerry Prince

Department of Electrical and Computer Engineering
Johns Hopkins University, USA

Abstract. Producing spatial transformations that are diffeomorphic has been a central problem in deformable image registration. As a diffeomorphic transformation should have positive Jacobian determinant $|J|$ everywhere, the number of voxels with $|J| < 0$ has been used to test for diffeomorphism and also to measure the irregularity of the transformation. For digital transformations, $|J|$ is commonly approximated using central difference, but this strategy can yield positive $|J|$'s for transformations that are clearly not diffeomorphic—even at the voxel resolution level. To show this, we first investigate the geometric meaning of different finite difference approximations of $|J|$. We show that to determine diffeomorphism for digital images, use of any individual finite difference approximations of $|J|$ is insufficient. We show that for a 2D transformation, four unique finite difference approximations of $|J|$'s must be positive to ensure the entire domain is invertible and free of folding at the pixel level. We also show that in 3D, ten unique finite differences approximations of $|J|$'s are required to be positive. Our proposed *digital diffeomorphism* criteria solves several errors inherent in the central difference approximation of $|J|$ and accurately detects non-diffeomorphic digital transformations.

Keywords: Deformable Image Registration · Digital Diffeomorphism · Finite Difference · Interpolation · Jacobian Determinants

1 Introduction

The goal of deformable image registration is to establish a nonlinear spatial transformation that aligns two images. For many tasks, it is reasonable to assume that the anatomy in the two images share the same topology. Therefore, for deformable registration algorithms, the ability to produce a topology preserving transformation is preferred. Following the work of Christensen *et al.* [7], many registration algorithms constrain the output transformations to be diffeomorphic to preserve topology [2,9]. In the continuous domain, a diffeomorphic transformation is a smooth and invertible mapping with a smooth inverse that is guaranteed to maintain the topology of the anatomy being transformed. Since a diffeomorphic transformation should have positive Jacobian determinant $|J|$ everywhere, testing if a transformation is diffeomorphic involves local computation of $|J|$. When a transformation is not diffeomorphic, it is common to use the number of

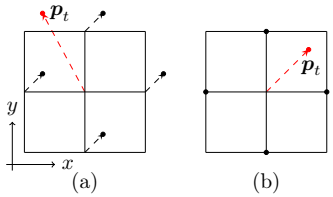

Fig. 1. (a) is an illustration of the *checkerboard problem* for $D^{0x}D^{0y}|J|$. (b) is a transformation that illustrates the inconsistency issue between $D^{-x}D^{-y}|J|$ and $D^{+x}D^{+y}|J|$. The transformation at each point is visualized as a displacement (shown as dotted arrow) and the displacement for the center point is highlighted in red.

voxels with negative $|J|$ [3,5,6,18] or the standard deviation of the logarithmic transformed $|J|$ [12,15,14] to measure the irregularity of the transformation.

Given a digital transformation that is defined on a regular grid, a widely accepted practice for computing the Jacobian is to use finite difference approximations of spatial derivatives. Along each axis, there are three commonly used methods for computing finite differences. We denote the forward, backward, and central differences that operate along the x axis (and similarly for the y and z axes) as $\mathcal{D}^{+x}$, $\mathcal{D}^{-x}$, and $\mathcal{D}^{0x}$, respectively. To approximate $|J|$ in 2D or 3D transformations, either the same or a different type of finite difference can be used for each axis. We denote the central difference approximations of $|J|$ in 2D and 3D as $\mathcal{D}^{0x}\mathcal{D}^{0y}|J|$ and $\mathcal{D}^{0x}\mathcal{D}^{0y}\mathcal{D}^{0z}|J|$, respectively. However, this very commonly used approach does not always work as expected. For example, Figure 1(a) shows a transformation around p that is not diffeomorphic despite the fact that $\mathcal{D}^{0x}\mathcal{D}^{0y}|J| = 1$. In fact, the transformation at $\boldsymbol{p}$ has no effect on the computation of $\mathcal{D}^{0x}\mathcal{D}^{0y}|J|(\boldsymbol{p})$, even if $\boldsymbol{p}$ moves outside the field of view. We call this the *checkerboard problem* because the Jacobian computations on the transformations of the "black" and "white" pixels (of a checkerboard) are independent of each other. A possible solution to this problem is to use $\mathcal{D}^{-x}\mathcal{D}^{-y}|J|$ or $\mathcal{D}^{+x}\mathcal{D}^{+y}|J|$ instead. However, Fig. 1(b) shows an example in which $\mathcal{D}^{-x}\mathcal{D}^{-y}|J|$ and $\mathcal{D}^{+x}\mathcal{D}^{+y}|J|$ have opposite signs, leading to contradictory conclusions. Therefore, determining if a digital transformation is diffeomorphic is a non-trivial task.

In this work, we first investigate the geometric meaning of finite difference approximations of $|J|$. We show that when using forward or backward differences, the sign of $|J|(\boldsymbol{p})$ determines if the underlying transformation $\mathcal{T}$ is invertible and orientation-preserving in a triangle (2D) or tetrahedron (3D) adjacent to $\boldsymbol{p}$. Reversing the orientation indicates folding in space. We formally define digital transformations that are globally invertible and free of folding as digital diffeomorphisms. In order to determine if a transformation is a digital diffeomorphism, at each point it is necessary to consider four finite difference approximated $|J|$'s for 2D transformations and ten $|J|$'s for 3D transformations. We also demonstrate that because of the *checkerboard problem* and other errors that are inherent in the central difference based $|J|$, it always underestimates the number of non-diffeomorphic voxels, which can lead to misleading comparisons between al-

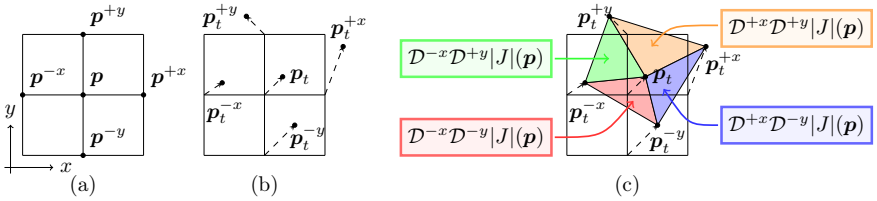

Fig. 2. (a) and (b) show the notations for each point around $\boldsymbol{p}$ and $\boldsymbol{p}_t$. (c) shows the triangular regions and their corresponding forward and backward difference based $|J|$'s.

gorithms. Finally, we propose to use non-diffeomorphic area (2D) and volume (3D) as more meaningful measurements of irregularity in computed transformations.

2 Methodology

2.1 Backward Difference Based Jacobian Determinant in 2D

Consider the standard Euclidean space $\mathbb{R}^2$ that follows the right-hand rule. Let $\mathcal{T}$ be a digital transformation for $\mathbb{R}^2$ that is defined for every grid point $\boldsymbol{p}$. When using backward differences on both x and y axes for approximating $|J|$ at point $\boldsymbol{p}$, we have

$$\mathcal{D}^{-x}\mathcal{D}^{-y}|J|(\boldsymbol{p}) = \begin{vmatrix} \mathcal{D}^{-x}\mathcal{T}_x(\boldsymbol{p}) & \mathcal{D}^{-y}\mathcal{T}_x(\boldsymbol{p}) \\ \mathcal{D}^{-x}\mathcal{T}_y(\boldsymbol{p}) & \mathcal{D}^{-y}\mathcal{T}_y(\boldsymbol{p}) \end{vmatrix}, \tag{1}$$

where $\mathcal{T}_x(\boldsymbol{p})$ and $\mathcal{T}_y(\boldsymbol{p})$ are the x and y components of $\mathcal{T}(\boldsymbol{p})$.

In this section, we denote the 4-connected-neighbors of $\boldsymbol{p}$ as $\boldsymbol{p}^{-x}, \boldsymbol{p}^{+x}, \boldsymbol{p}^{-y}$, and $\boldsymbol{p}^{+y}$, as shown in Fig. 2(a). The transformed locations are denoted with subscripts t (see Fig. 2(b)), for example $\boldsymbol{p}_t^{+x} := \mathcal{T}(\boldsymbol{p}^{+x})$. We further denote the triangular region defined by the vectors $\boldsymbol{p}\boldsymbol{p}^{-x}$ and $\boldsymbol{p}\boldsymbol{p}^{-y}$ as $\triangle\boldsymbol{p}\boldsymbol{p}^{-x}\boldsymbol{p}^{-y}$, and we assume that the 2D transformation $\mathcal{T}$ is linearly interpolated on $\triangle\boldsymbol{p}\boldsymbol{p}^{-x}\boldsymbol{p}^{-y}$.

Proposition 1. *A 2D transformation $\mathcal{T}$ is invertible for $\triangle\boldsymbol{p}\boldsymbol{p}^{-x}\boldsymbol{p}^{-y}$ if and only if $\mathcal{D}^{-x}\mathcal{D}^{-y}|J|(\boldsymbol{p})$ for $\mathcal{T}$ is nonzero.*

Proof. Since $\mathcal{T}$ is linearly interpolated on $\triangle\boldsymbol{p}\boldsymbol{p}^{-x}\boldsymbol{p}^{-y}$, $\mathcal{T}$ is linear for $\triangle\boldsymbol{p}\boldsymbol{p}^{-x}\boldsymbol{p}^{-y}$ and can be written as a 2×2 matrix with $\boldsymbol{p}_t\boldsymbol{p}_t^{-x}$ and $\boldsymbol{p}_t\boldsymbol{p}_t^{-y}$ as its columns. Thus, $\mathcal{T}$ is invertible if and only if $\boldsymbol{p}_t\boldsymbol{p}_t^{-x}$ and $\boldsymbol{p}_t\boldsymbol{p}_t^{-y}$ are linearly independent (not colinear). $\mathcal{D}^{-x}\mathcal{D}^{-y}|J|(\boldsymbol{p})$ can be written as a triple product:

$$\mathcal{D}^{-x}\mathcal{D}^{-y}|J|(\boldsymbol{p}) = (\boldsymbol{p}_t\boldsymbol{p}_t^{-x} \times \boldsymbol{p}_t\boldsymbol{p}_t^{-y}) \cdot \boldsymbol{n}, \tag{2}$$

where $\boldsymbol{n}$ is the unit vector perpendicular to vectors $\boldsymbol{p}_t\boldsymbol{p}_t^{-x}$ and $\boldsymbol{p}_t\boldsymbol{p}_t^{-y}$ and is positively oriented following the right-hand rule. Therefore, $\mathcal{T}$ is invertible if and only if $\mathcal{D}^{-x}\mathcal{D}^{-y}|J|(\boldsymbol{p}) \neq 0$. ∎

Definition 1. *A 2D transformation $\mathcal{T}$ is said to cause folding of $\triangle\boldsymbol{p}\boldsymbol{p}^{-x}\boldsymbol{p}^{-y}$ if the orientation of $\triangle\boldsymbol{p}\boldsymbol{p}^{-x}\boldsymbol{p}^{-y}$ is reversed by $\mathcal{T}$.*

Proposition 2. *A 2D transformation $\mathcal{T}$ is free of folding for $\triangle \boldsymbol{p}\boldsymbol{p}^{-x}\boldsymbol{p}^{-y}$ if and only if $\mathcal{D}^{-x}\mathcal{D}^{-y}\left|J\right|(\boldsymbol{p})$ for $\mathcal{T}$ is positive.*

Proof. By the right-hand rule, $\triangle \boldsymbol{p}\boldsymbol{p}^{-x}\boldsymbol{p}^{-y}$ is positively oriented. ($\Rightarrow$) When $\mathcal{T}$ is free of folding, the orientation of $\triangle \boldsymbol{p}\boldsymbol{p}^{-x}\boldsymbol{p}^{-y}$ is preserved by $\mathcal{T}$. Because of linear interpolation, $\triangle \boldsymbol{p}\boldsymbol{p}^{-x}\boldsymbol{p}^{-y}$ is transformed to $\triangle \boldsymbol{p}_t\boldsymbol{p}_t^{-x}\boldsymbol{p}_t^{-y}$, which is also positively oriented. Equation 2 shows $\mathcal{D}^{-x}\mathcal{D}^{-y}|J|(\boldsymbol{p})$ equals twice the signed area of $\triangle \boldsymbol{p}_t\boldsymbol{p}_t^{-x}\boldsymbol{p}_t^{-y}$. Therefore, $\mathcal{D}^{-x}\mathcal{D}^{-y}|J|(\boldsymbol{p}) > 0$. ($\Leftarrow$) When $\mathcal{D}^{-x}\mathcal{D}^{-y}|J|(\boldsymbol{p}) > 0$, from Eq. 2 $\triangle \boldsymbol{p}_t\boldsymbol{p}_t^{-x}\boldsymbol{p}_t^{-y}$ is positively oriented. Because of linear interpolation, $\triangle \boldsymbol{p}\boldsymbol{p}^{-x}\boldsymbol{p}^{-y}$ is transformed to $\triangle \boldsymbol{p}_t\boldsymbol{p}_t^{-x}\boldsymbol{p}_t^{-y}$ and both of them are positively oriented. Therefore, $\mathcal{T}$ is free of folding for $\triangle \boldsymbol{p}\boldsymbol{p}^{-x}\boldsymbol{p}^{-y}$. ∎

Definition 2. *A 2D transformation $\mathcal{T}$ is digitally diffeomorphic for the region $\triangle \boldsymbol{p}\boldsymbol{p}^{-x}\boldsymbol{p}^{-y}$ if $\mathcal{T}$ is invertible and free of folding for $\triangle \boldsymbol{p}\boldsymbol{p}^{-x}\boldsymbol{p}^{-y}$.*

Proposition 3. *A 2D transformation $\mathcal{T}$ is digitally diffeomorphic for the region $\triangle \boldsymbol{p}\boldsymbol{p}^{-x}\boldsymbol{p}^{-y}$ if and only if $\mathcal{D}^{-x}\mathcal{D}^{-y}\left|J\right|(\boldsymbol{p}) > 0$.*

Proof. Proposition 3 is a direct consequence of Propositions 1 and 2. ∎

In conclusion, $\mathcal{D}^{-x}\mathcal{D}^{-y}\left|J\right|$ for point $\boldsymbol{p}$ informs us about the digitally diffeomorphic property of a triangle adjacent to $\boldsymbol{p}$, under the assumption that the transformation is linearly interpolated.

2.2 Digital Diffeomorphism in Two Dimensions

Similar to $\mathcal{D}^{-x}\mathcal{D}^{-y}|J|(\boldsymbol{p})$, we can replicate Proposition 3 to establish that any $|J|(\boldsymbol{p})$ approximated using any combination of forward and backward differences is testing if the transformation is digitally diffeomorphic for a triangular region around $\boldsymbol{p}$ (see Fig. 2(c)), assuming that the region is linearly interpolated. Since these $|J|(\boldsymbol{p})$'s cover different regions, their signs are independent of each other. For example, $\mathcal{T}$ can have a positive $\mathcal{D}^{-x}\mathcal{D}^{-y}|J|(\boldsymbol{p})$ and a negative $\mathcal{D}^{+x}\mathcal{D}^{+y}|J|(\boldsymbol{p})$ at the same time (see Fig. 1(b)). For each of these $|J|$, the triangular regions of all $\boldsymbol{p}$'s only cover half of the space (*e.g.,* $\mathcal{D}^{-x}\mathcal{D}^{-y}|J|$ only considers the red tiles in Fig. 3(a)). Consequently, even if a transformation $\mathcal{T}$ has $\mathcal{D}^{-x}\mathcal{D}^{-y}|J|(\boldsymbol{p}) > 0$ for all $\boldsymbol{p}$'s, half the space is not considered and can potentially exhibit folding or be non-invertible. This is also the case for other forward and backward difference computations of $|J|$.

Definition 3. *A 2D digital transformation $\mathcal{T}$ is a digital diffeomorphism if for every grid point $\boldsymbol{p}$ it has $\mathcal{D}^{-x}\mathcal{D}^{-y}|J|(\boldsymbol{p}) > 0$, $\mathcal{D}^{-x}\mathcal{D}^{+y}|J|(\boldsymbol{p}) > 0$, $\mathcal{D}^{+x}\mathcal{D}^{-y}|J|(\boldsymbol{p}) > 0$, and $\mathcal{D}^{+x}\mathcal{D}^{+y}|J|(\boldsymbol{p}) > 0$.*

Although combining the triangular regions of $\mathcal{D}^{-x}\mathcal{D}^{-y}|J|$ and $\mathcal{D}^{+x}\mathcal{D}^{+y}|J|$ can cover the entire space, positive $\mathcal{D}^{-x}\mathcal{D}^{-y}|J|$ and $\mathcal{D}^{+x}\mathcal{D}^{+y}|J|$ only guarantee that the transformation is digitally diffeomorphic when the transformation is piecewise linearly interpolated as shown in Fig. 3(a). A different choice, for example shown in Fig. 3(b), which correspond to $\mathcal{D}^{-x}\mathcal{D}^{+y}|J|$ and $\mathcal{D}^{+x}\mathcal{D}^{-y}|J|$

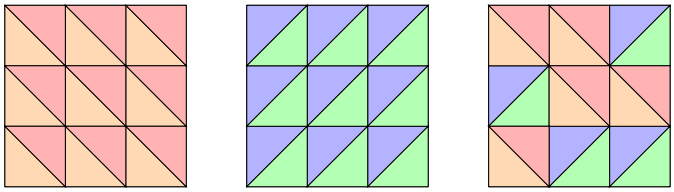

Fig. 3. Illustration of the combinations of Jacobian determinants and the corresponding triangular regions. (a) $\mathcal{D}^{-x}\mathcal{D}^{-y}|J|(\boldsymbol{p})$ and $\mathcal{D}^{+x}\mathcal{D}^{+y}|J|(\boldsymbol{p})$. (b) $\mathcal{D}^{-x}\mathcal{D}^{+y}|J|(\boldsymbol{p})$ and $\mathcal{D}^{+x}\mathcal{D}^{-y}|J|(\boldsymbol{p})$. (c) Each pixel uses different Jacobian determinants.

can give contradictory conclusions. Since there are two ways of dividing the square-size area in-between grid points, there are many more piecewise linear transformations that correspond to the same digital transformation, *e.g.,* Fig. 3(c). The proposed digital diffeomorphism guarantees the transformation to be free of folding and invertible regardless of the piecewise linear transformation that is used.

2.3 Central Difference Based Jacobian Determinant

Definition 4. *For a given transformation $\mathcal{T}$ and a grid point $\boldsymbol{p}$, $\mathcal{R} \subseteq \mathbb{R}^2$ is the feasible region for $\boldsymbol{p}_t$ such that all the forward and backward difference based $|J|$'s of $\boldsymbol{p}$ are positive.*

Proposition 4. *$\mathcal{R}$ is the intersection of four half-planes that are specified as the left side of four vectors $\boldsymbol{p}_t^{-x}\boldsymbol{p}_t^{-y}$, $\boldsymbol{p}_t^{-y}\boldsymbol{p}_t^{+x}$, $\boldsymbol{p}_t^{+x}\boldsymbol{p}_t^{+y}$, and $\boldsymbol{p}_t^{+y}\boldsymbol{p}_t^{-x}$.*

Proof. Equation 1 can be written as: $\mathcal{D}^{-x}\mathcal{D}^{-y}|J|(\boldsymbol{p}) = (\boldsymbol{p}_t^{-x}\boldsymbol{p}_t^{-y} \times \boldsymbol{p}_t^{-x}\boldsymbol{p}_t) \cdot \boldsymbol{n}$. Therefore, for $\mathcal{D}^{-x}\mathcal{D}^{-y}|J|(\boldsymbol{p})$ to be positive, $\boldsymbol{p}_t$ must be on the left side of $\boldsymbol{p}_t^{-x}\boldsymbol{p}_t^{-y}$. Similarly for the other forward or backward difference based $|J|$'s. Thus, $\mathcal{R}$ is the intersection of four half-planes that are specified as the left side of the four vectors $\boldsymbol{p}_t^{-x}\boldsymbol{p}_t^{-y}$, $\boldsymbol{p}_t^{-y}\boldsymbol{p}_t^{+x}$, $\boldsymbol{p}_t^{+x}\boldsymbol{p}_t^{+y}$, and $\boldsymbol{p}_t^{+y}\boldsymbol{p}_t^{-x}$. ∎

Figure 4 shows examples of $\mathcal{R}$. In Figs. 4(c) and (d), no matter where $\boldsymbol{p}_t$ is located, at least one forward or backward difference based $|J|(\boldsymbol{p})$ is guaranteed to be negative and, thus, $\mathcal{R}$ is an empty set. This makes sense since the transformations in Figs. 4(c) and (d) cause folds in space.

Proposition 5. *Assume $\boldsymbol{p}_t^{-x}$, $\boldsymbol{p}_t^{-y}$, $\boldsymbol{p}_t^{+x}$, and $\boldsymbol{p}_t^{+x}$ forms a simple polygon (without self-intersection). Then $\mathcal{R}$ is non-empty if and only if $\mathcal{D}^{0x}\mathcal{D}^{0y}\,|J|\,(\boldsymbol{p}) > 0$.*

Proof. $\mathcal{D}^{0x}\mathcal{D}^{0y}|J|(\boldsymbol{p})$ can be written as:

$$\mathcal{D}^{0x}\mathcal{D}^{0y}|J| = \frac{1}{2}\left(\mathcal{D}^{-x}\mathcal{D}^{-y}|J| + \mathcal{D}^{+x}\mathcal{D}^{-y}|J| + \mathcal{D}^{-x}\mathcal{D}^{+y}|J| + \mathcal{D}^{+x}\mathcal{D}^{+y}|J|\right). \quad (3)$$

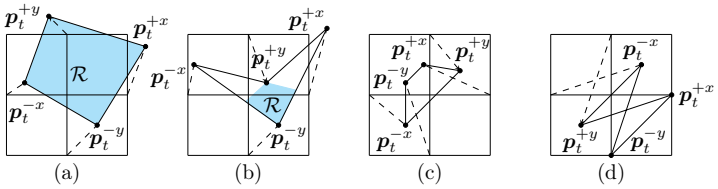

Fig. 4. Examples of $\mathcal{R}$ (shaded region) for $\boldsymbol{p}_t$ such that $\mathcal{T}$ is digitally diffeomorphic. (c) and (d) show examples of $\mathcal{T}$'s that are causing folds in and thus $\mathcal{R}$ is an empty set.

($\Rightarrow$) If $\mathcal{R}$ is non-empty, for every $\boldsymbol{p}_t \in \mathcal{R}$ we must have all the forward or backward differences based $|J|(\boldsymbol{p}) > 0$ and therefore from Eq. 3, $\mathcal{D}^{0x}\mathcal{D}^{0y}|J|(\boldsymbol{p}) > 0$. ($\Leftarrow$) On the other hand, if $\mathcal{D}^{0x}\mathcal{D}^{0y}|J| > 0$, the polygon $\boldsymbol{p}_t^{-x}\boldsymbol{p}_t^{-y}\boldsymbol{p}_t^{+x}\boldsymbol{p}_t^{+y}$ is positively oriented [4] (*i.e.* interior to the left). Thus, if there exists $\boldsymbol{p}_t$ that is visible to all vertices of the polygon, $\boldsymbol{p}_t \in \mathcal{R}$. It can be proved following [8] that such $\boldsymbol{p}_t$ always exists for simple polygons with less than or equal to five vertices. Therefore, $\mathcal{R}$ is non-empty. ∎

Although a positive $\mathcal{D}^{0x}\mathcal{D}^{0y}|J|(\boldsymbol{p})$ ensures $\mathcal{R}$ exists, $\boldsymbol{p}$ can still be digitally non-diffeomorphic when $\boldsymbol{p}_t \notin \mathcal{R}$, which results in the *checkerboard problem*. In addition to the *checkerboard problem*, $\mathcal{D}^{0x}\mathcal{D}^{0y}|J|$ also fails to provide a meaningful interpretation when the polygon $\boldsymbol{p}_t^{-x}\boldsymbol{p}_t^{-y}\boldsymbol{p}_t^{+x}\boldsymbol{p}_t^{+y}$ exhibits self-intersection (see Fig. 4(d)). In conclusion, $\mathcal{D}^{0x}\mathcal{D}^{0y}|J|(\boldsymbol{p}) < 0$ always indicates that $\mathcal{T}$ is digitally non-diffeomorphic but $\mathcal{D}^{0x}\mathcal{D}^{0y}|J|(\boldsymbol{p}) > 0$ does not mean it is digitally diffeomorphic because of the checkerboard or self-intersection problems. Therefore, central difference based $|J|$ always underestimate digital non-diffeomorphism.

2.4 Digital Diffeomorphism in Three Dimensions

Consider the standard Euclidean space $\mathbb{R}^3$ that follows the right-hand rule. Let $\mathcal{T}$ be a digital transformation for $\mathbb{R}^3$ that is defined for every grid point $\boldsymbol{p}$. We denote the 6-connected-neighbors of $\boldsymbol{p}$ as $\boldsymbol{p}^{\pm x}, \boldsymbol{p}^{\pm y}, \boldsymbol{p}^{\pm z}$ (shown in Fig. 5(a)) and the transformed locations with subscripts t. We further denote the tetrahedron region defined by the vectors $\boldsymbol{p}\boldsymbol{p}^{-x}$, $\boldsymbol{p}\boldsymbol{p}^{-y}$, and $\boldsymbol{p}\boldsymbol{p}^{-z}$ as $\triangle\boldsymbol{p}\boldsymbol{p}^{-x}\boldsymbol{p}^{-y}\boldsymbol{p}^{-z}$, and we assume that the 3D transformation $\mathcal{T}$ is linearly interpolated on $\triangle\boldsymbol{p}\boldsymbol{p}^{-x}\boldsymbol{p}^{-y}\boldsymbol{p}^{-z}$.

Proposition 6. *A 3D transformation $\mathcal{T}$ is invertible for $\triangle\boldsymbol{p}\boldsymbol{p}^{-x}\boldsymbol{p}^{-y}\boldsymbol{p}^{-z}$ if and only if $\mathcal{D}^{-x}\mathcal{D}^{-y}\mathcal{D}^{-z}|J|$ for $\boldsymbol{p}$ is nonzero.*

Proof. Since $\mathcal{T}$ is linearly interpolated on $\triangle\boldsymbol{p}\boldsymbol{p}^{-x}\boldsymbol{p}^{-y}\boldsymbol{p}^{-z}$, $\mathcal{T}$ is linear for $\triangle\boldsymbol{p}\boldsymbol{p}^{-x}\boldsymbol{p}^{-y}\boldsymbol{p}^{-z}$ and can be written as a 3×3 matrix with $\boldsymbol{p}_t\boldsymbol{p}_t^{-x}$, $\boldsymbol{p}_t\boldsymbol{p}_t^{-y}$, and $\boldsymbol{p}_t\boldsymbol{p}^{-z}$ as its columns. Thus, $\mathcal{T}$ is invertible if and only if $\boldsymbol{p}_t\boldsymbol{p}_t^{-x}$, $\boldsymbol{p}_t\boldsymbol{p}_t^{-y}$, and $\boldsymbol{p}_t\boldsymbol{p}^{-z}$ are linearly independent (not colinear). $\mathcal{D}^{-x}\mathcal{D}^{-y}\mathcal{D}^{-z}|J|(\boldsymbol{p})$ can be written as a triple product:

$$\mathcal{D}^{-x}\mathcal{D}^{-y}\mathcal{D}^{-z}|J|(\boldsymbol{p}) = -(\boldsymbol{p}_t\boldsymbol{p}_t^{-x} \times \boldsymbol{p}_t\boldsymbol{p}_t^{-y}) \cdot \boldsymbol{p}_t\boldsymbol{p}_t^{-z}. \tag{4}$$

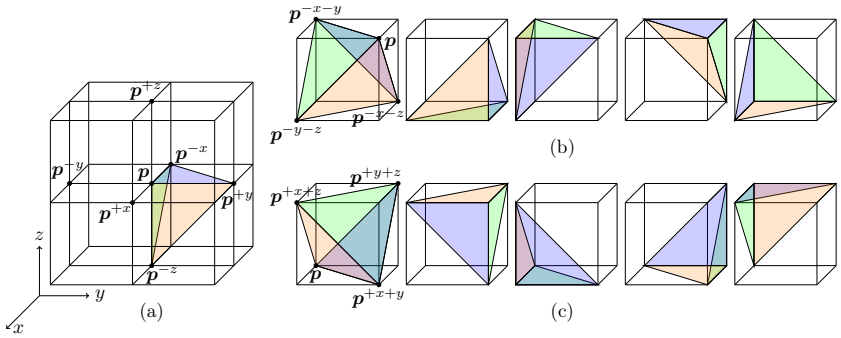

Fig. 5. (a) shows the notations for point $\boldsymbol{p}$ and its neighbors in 3D and the tetrahedron considered by $\mathcal{D}^{-x}\mathcal{D}^{+y}\mathcal{D}^{-z}|J|$. (b) is an illustration of the two schemes to divide the cube volume in between grid points in 3D.

Therefore, $\mathcal{T}$ is invertible if and only if $\mathcal{D}^{-x}\mathcal{D}^{-y}\mathcal{D}^{-z}|J|(\boldsymbol{p}) \neq 0$. ∎

Definition 5. *A 3D transformation $\mathcal{T}$ is said to cause folding for $\triangle \boldsymbol{p}\boldsymbol{p}^{-x}\boldsymbol{p}^{-y}\boldsymbol{p}^{-z}$ if the orientation of $\triangle \boldsymbol{p}\boldsymbol{p}^{-x}\boldsymbol{p}^{-y}\boldsymbol{p}^{-z}$ is reversed by $\mathcal{T}$.*

Proposition 7. *A 3D transformation $\mathcal{T}$ is free of folding for $\triangle \boldsymbol{p}\boldsymbol{p}^{-x}\boldsymbol{p}^{-y}\boldsymbol{p}^{-z}$ if and only if $\mathcal{T}$ has $\mathcal{D}^{-x}\mathcal{D}^{-y}\mathcal{D}^{-z}|J|(\boldsymbol{p}) > 0$.*

Proof. ($\Rightarrow$) When $\mathcal{T}$ is free of folding, the orientation of $\triangle \boldsymbol{p}\boldsymbol{p}^{-x}\boldsymbol{p}^{-y}\boldsymbol{p}^{-z}$ (negatively oriented by the right-hand rule) is preserved by $\mathcal{T}$. Because of linear interpolation, $\triangle \boldsymbol{p}\boldsymbol{p}^{-x}\boldsymbol{p}^{-y}\boldsymbol{p}^{-z}$ is transformed to $\triangle \boldsymbol{p}_t\boldsymbol{p}_t^{-x}\boldsymbol{p}_t^{-y}\boldsymbol{p}_t^{-z}$, which is also negatively oriented. Equation 4 shows $\mathcal{D}^{-x}\mathcal{D}^{-y}\mathcal{D}^{-z}|J|(\boldsymbol{p})$ equals to six times the negative signed volume of $\triangle \boldsymbol{p}_t\boldsymbol{p}_t^{-x}\boldsymbol{p}_t^{-y}\boldsymbol{p}_t^{-z}$. Therefore, $\mathcal{D}^{-x}\mathcal{D}^{-y}\mathcal{D}^{-z}|J|(\boldsymbol{p}) > 0$. ($\Leftarrow$) On the other hand, $\mathcal{D}^{-x}\mathcal{D}^{-y}\mathcal{D}^{-z}|J|(\boldsymbol{p}) > 0$ indicates that $\triangle \boldsymbol{p}_t\boldsymbol{p}_t^{-x}\boldsymbol{p}_t^{-y}\boldsymbol{p}_t^{-z}$ is negatively oriented by Eq. 4. Because of linear interpolation $\triangle \boldsymbol{p}\boldsymbol{p}^{-x}\boldsymbol{p}^{-y}\boldsymbol{p}^{-z}$ is mapped to $\triangle \boldsymbol{p}_t\boldsymbol{p}_t^{-x}\boldsymbol{p}_t^{-y}\boldsymbol{p}_t^{-z}$ and both of them are negatively oriented. Therefore, $\mathcal{T}$ is free of folding for $\triangle \boldsymbol{p}\boldsymbol{p}^{-x}\boldsymbol{p}^{-y}\boldsymbol{p}^{-z}$. ∎

Definition 6. *A 3D transformation $\mathcal{T}$ is digitally diffeomorphic for the region $\triangle \boldsymbol{p}\boldsymbol{p}^{-x}\boldsymbol{p}^{-y}\boldsymbol{p}^{-z}$ if $\mathcal{T}$ is invertible and free of folding for $\triangle \boldsymbol{p}\boldsymbol{p}^{-x}\boldsymbol{p}^{-y}\boldsymbol{p}^{-z}$.*

Proposition 8. *A 3D transformation $\mathcal{T}$ is digitally diffeomorphic for the region $\triangle \boldsymbol{p}\boldsymbol{p}^{-x}\boldsymbol{p}^{-y}\boldsymbol{p}^{-z}$ if and only if $\mathcal{D}^{-x}\mathcal{D}^{-y}\mathcal{D}^{-z}|J|(\boldsymbol{p}) > 0$.*

Proof. Proposition 8 is a direct consequence of Propositions 6 and 7. ∎

Similarly, we can prove that a $|J|(\boldsymbol{p})$ approximated using any combinations of forward and backward differences is testing if the transformation is digitally diffeomorphic in a tetrahedron adjacent to $\boldsymbol{p}$. One of these tetrahedra (for $\mathcal{D}^{-x}\mathcal{D}^{+y}\mathcal{D}^{-z}|J|$) are visualized in Fig. 5(a). However, unlike the 2D case where

all the triangular regions completely cover the entire 2D space, the union of all these adjacent tetrahedra does not fill the entire 3D space. Therefore, even if all forward and backward difference approximations of $|J|$ are positive, the transformation can still cause folding in the spaces not covered by these adjacent tetrahedra.

To solve this issue, we introduce another tetrahedron $\triangle \boldsymbol{p}\boldsymbol{p}^{-x-y}\boldsymbol{p}^{-x-z}\boldsymbol{p}^{-y-z}$, as shown in Fig. 5(b). When combined with four existing tetrahedra from finite difference based $|J|$'s, they completely cover the entire volume. Define $|J_1^\star|(\boldsymbol{p})$ as

$$|J_1^\star|(\boldsymbol{p}) = (\boldsymbol{p}_t\boldsymbol{p}_t^{-x-y} \times \boldsymbol{p}_t\boldsymbol{p}_t^{-x-z}) \cdot \boldsymbol{p}_t\boldsymbol{p}_t^{-y-z}, \tag{5}$$

where $\boldsymbol{p}_t^{-x-y}$, $\boldsymbol{p}_t^{-x-z}$, and $\boldsymbol{p}_t^{-y-z}$ are the transformed locations of $\boldsymbol{p}^{-x-y}$, $\boldsymbol{p}^{-x-z}$, $\boldsymbol{p}^{-y-z}$. The signed volume of the extra tetrahedron equals $\frac{1}{6}|J_1^\star|(\boldsymbol{p})$ after applying $\mathcal{T}$. Similar to 2D, there are two ways of dividing the cube-size volume in-between grid points into five tetrahedra, as shown in Figs. 5(b) and (c). The signed volume of the extra tetrahedron in Fig. 5(c) can be computed as $\frac{1}{6}|J_2^\star|(\boldsymbol{p})$, where

$$|J_2^\star|(\boldsymbol{p}) = (\boldsymbol{p}_t\boldsymbol{p}_t^{+x+y} \times \boldsymbol{p}_t\boldsymbol{p}_t^{+y+z}) \cdot \boldsymbol{p}_t\boldsymbol{p}_t^{+x+z}. \tag{6}$$

Definition 7. *A 3D digital transformation $\mathcal{T}$ is a digital diffeomorphism if for every grid point $\boldsymbol{p}$ its forward and backward difference based $|J|$'s of $\boldsymbol{p}$ are all positive and both $|J_1^\star|(\boldsymbol{p})$ and $|J_2^\star|(\boldsymbol{p})$ are positive.*

The central difference approximation of $|J|$ in 3D calculates the signed volume of an octahedron with vertices $\boldsymbol{p}_t^{-x}\boldsymbol{p}_t^{+x}\boldsymbol{p}_t^{-y}\boldsymbol{p}_t^{+y}\boldsymbol{p}_t^{-z}\boldsymbol{p}_t^{+z}$ when the octahedron is simple. The proof is a straightforward extension of Eq. 3. It is easy to show that $\mathcal{D}^{0x}\mathcal{D}^{0y}\mathcal{D}^{0z}|J|$ can also have the checkerboard problem or the self-intersection problem as in the 2D case. Note that Proposition 5 cannot be generalized to 3D because $\boldsymbol{p}_t^{-x}\boldsymbol{p}_t^{+x}\boldsymbol{p}_t^{-y}\boldsymbol{p}_t^{+y}\boldsymbol{p}_t^{-z}\boldsymbol{p}_t^{+z}$ may not be tetrahedralizable [20] and thus, $\mathcal{D}^{0x}\mathcal{D}^{0y}\mathcal{D}^{0z}|J|(\boldsymbol{p}) > 0$ cannot guarantee $\mathcal{R}$ in 3D is non-empty.

2.5 Non-diffeomorphic Volume and Area

For non-diffeomorphic transformations in 3D, the number and percentage of non-diffeomorphic voxels are often used to measure its irregularity. Specifically, a voxel is considered non-diffeomorphic if its center location $\boldsymbol{p}$ has $\mathcal{D}^{0x}\mathcal{D}^{0y}\mathcal{D}^{0z}|J|(\boldsymbol{p}) \leq 0$. We have shown that forward and backward difference approximations of $|J|(\boldsymbol{p})$ test the digital diffeomorphism of tetrahedra adjacent to $\boldsymbol{p}$. Therefore, we report the number and percentage of non-diffeomorphic tetrahedra (NDT) as additional quality measures. However, none of these quantities capture the *volume* of digitally non-diffeomorphic regions in the warped image. Therefore, we propose and also report the average non-diffeomorphic volume (NDV), computed as

$$\text{NDV} = -\frac{1}{2}\sum_{\boldsymbol{p}}\left[\frac{\min(|J_1^\star|(\boldsymbol{p}),0)}{6} + \frac{\min(|J_2^\star|(\boldsymbol{p}),0)}{6} + \sum_{i=1}^{8}\frac{\min(|J_i|(\boldsymbol{p}),0)}{6}\right], \tag{7}$$

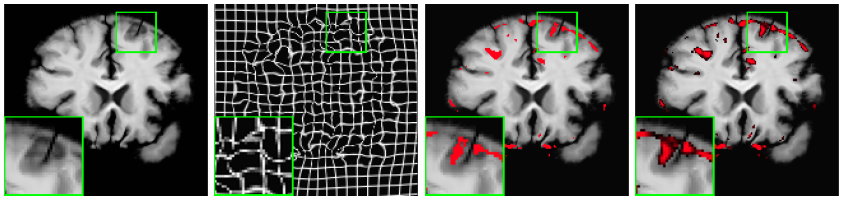

(a) (b) (c) (d)

Fig. 6. A visualization of the proposed non-diffeomorphic area (only the displacement inside the coronal plane was considered in this example). (a) The warped image. (b) The grid line representation of the transformation. (c) The warped image with non-diffeomorphic pixels (measured by $\mathcal{D}^{0x}\mathcal{D}^{0y}|J|$) highlighted in red. (d) The warped image with a map overlay indicating the non-diffeomorphic area.

where $|J_i|, i \in [1, \ldots, 8]$, are the Jacobian determinants approximated using the eight possible combinations of forward and backward differences and $|J_1^\star|$ and $|J_2^\star|$ are given above. In 2D, the area of the non-diffeomorphic regions in the warped image can be computed as the average non-diffeomorphic area (NDA),

$$\text{NDA} = -\frac{1}{2}\sum_{\boldsymbol{p}}\sum_{i=1}^{4}\frac{\min(|J_i|(\boldsymbol{p}), 0)}{2}, \tag{8}$$

where $|J_i|, i \in [1, \ldots, 4]$, are the Jacobian determinants approximated using the four possible combinations of forward and backward differences.

3 Experiments

We compared the proposed digital diffeomorphism and the commonly used $\mathcal{D}^{0x}\mathcal{D}^{0y}\mathcal{D}^{0z}|J|$ using several deformable registration algorithms on two publicly available datasets:

`IXI:` A total of 576 T1–weighted brain magnetic resonance images (MRIs) from the IXI dataset [1] were used. 403 scans were used in training for the task of atlas-to-subject registration [16] and 58 scans were used for validation. The transformations generated from registering the atlas brain MRI to 115 test scans were evaluated.

`Learn2Reg OASIS:` We also used the brain T1 MRIs from the 2021 Learn2Reg challenge [12,17]. Scans were preprocessed using FreeSurfer [10,13]. All algorithms were trained using the training set of 414 scans and the transformations for the 19 validation pairs were evaluated.

The central difference Jacobian determinant approximation was implemented directly from the 2021 Learn2Reg challenge evaluation script. The implementation details and hyper-parameters for each of the algorithms were adopted from [5] and [18]. The source code of this work is available at https://github.com/yihao6/digital_diffeomorphism.

Table 1. Results for the `IXI` dataset.

	$\mathcal{D}^{0x}\mathcal{D}^{0y}\mathcal{D}^{0z}\lvert J\rvert \leq 0$		Any $\lvert J_i\rvert \leq 0$		NDT	Proposed	
	voxel#	%	voxel#	%	%	NDV	%
MIDIR [21]	0.0 ± 0.0	0.00%	0.1 ± 0.7	0.00%	0.00%	0.0 ± 0.0	0.00%
Cyclemorph [16]	44126.5 ±8526.4	2.83%	99560.0 ±16833.8	6.38%	3.38%	17923.6 ±3083.3	1.15%
Voxelmorph [3]	41233.1 ±8091.3	2.64%	98241.0 ±17061.1	6.26%	3.23%	16261.5 ±2709.3	1.04%
Transmorph [5]	35324.1 ±7887.7	2.26%	88263.1 ±17261.7	5.65%	2.82%	14034.7 ±2902.5	0.90%
im2grid [18]	8291.4 ±5928.4	0.53%	20282.7 ±7853.8	1.3%	0.66%	822.6 ±248.5	0.05%
deedsBCV [11]	5704.7 ±1939.6	0.37%	12212.9 ±3118.1	0.79%	0.46%	1597.4 ±661.5	0.10%
NiftyReg [19]	222.2 ±776.1	0.01%	288.9 ±945.7	0.02%	0.01%	10.9 ±45.4	0.00%

The results for the two datasets are summarized in Tables 1 and 2. All the percentages were calculated relative to the brain volume of the fixed image. For $\mathcal{D}^{0x}\mathcal{D}^{0y}\mathcal{D}^{0z}|J|$, we calculated the number of non-diffeomorphic voxels (voxel#) and its percentage (%). We also report the number (and percentage) of voxels that have at least one $|J_i| \leq 0$, denoted as 'Any $|J_i| \leq 0$'. We observe that in most of the cases, there are actually more than twice the number of voxels having $|J_i| \leq 0$ for some finite difference than that found using only the central difference. The differences between '$\mathcal{D}^{0x}\mathcal{D}^{0y}\mathcal{D}^{0z}|J| \leq 0$' and 'Any $|J_i| \leq 0$' highlight that the errors from the central difference approximation are very common in practice.

The percentage of non-diffeomorphic tetrahedra (NDT), the proposed average non-diffeomorphic volume (NDV) and its percentage are shown in the last three columns of Tables 1 and 2. For algorithms that impose strong regularization on the transformations (*e.g., MIDIR* [21], *deedsBCV* [11], *NiftyReg* [19], and *SyN* [2]), a small NDV is observed. On the other hand, deep learning methods [16,3,5,18] that directly output deformation fields usually have higher NDVs. The NDV generally follows the trends of other measurements but different behaviors can also be observed. For example, *im2grid* [18] on the `Learn2Reg OASIS` dataset has a higher percentage of non-diffeomorphic tetrahedra compared with *Voxelmorph* [3], but the resultant non-diffeomorphic volume is much smaller for *im2grid*. This suggests that the transformations produced by *im2grid* are closer to be digitally diffeomorphic than *Voxelmorph*. Note that the results shown in Tables 1 and 2 do not reflect the accuracy of the algorithms.

A visualization of results from the `IXI` dataset is shown in Fig. 6. Since it is difficult to visualize displacements across slices (anterior-posterior direction), only the displacements within the coronal plane were considered. Thus, we computed the non-diffeomorphic area instead of non-diffeomorphic volume. For each pixel in Fig. 6(d), a higher red intensity indicates larger non-diffeomorphic area around that pixel. The non-diffeomorphic pixels computed from $\mathcal{D}^{0x}\mathcal{D}^{0y}|J|$ are highlighted in Fig. 6(c) for comparison.

Table 2. Results for the `Learn2Reg OASIS` dataset.

	$\mathcal{D}^{0x}\mathcal{D}^{0y}\mathcal{D}^{0z}\lvert J\rvert \leq 0$		Any $\lvert J_i\rvert \leq 0$		NDT	Proposed	
	voxel#	%	voxel#	%	%	NDV	%
SyN [2]	205.5 ±331.1	0.01%	278.2 ±415.3	0.02%	0.02%	85.0 ±204.1	0.01%
im2grid [18]	22905.6 ±4142.3	1.61%	161071.8 ±18271.5	11.36%	3.79%	8774.7 ±975.6	0.62%
Voxelmorph [3]	40418.4 ±8991.3	2.84%	94343.8 ±18452.7	6.64%	3.47%	18448.2 ±4319.0	1.30%
Transmorph [5]	31646.6 ±7609	2.22%	78533.7 ±16113.0	5.52%	2.76%	13502.7 ±3779.9	0.95%

4 Discussion

The Jacobian determinant of transformations is a widely used metric in deformable image registration, but the details of its computation are often overlooked. In this paper, we focused on the finite difference based approximation of $|J|$. Contrary to what one might expect, the commonly used central difference based $|J|$ does not reflect if the transformation is diffeomorphic or not. We proposed the definition of digital diffeomorphism that solves several errors that are inherent in the central difference based $|J|$. We further propose to use non-diffeomorphic volume to measure the irregularity of 3D transformations.

Our analysis shows that for the finite difference based $|J|$'s to be meaningful, the digital transformations are assumed to be piecewise linear. Since these transformations are not differentiable on the edges of triangles (2D) or tetrahedra (3D), the proposed digital diffeomorphism is different from the diffeomorphism in the continuous domain. The relationship between the two concepts needs to be investigated in future work. In addition to the proposed non-diffeomorphic area and non-diffeomorphic volume, there are many more measurements that can be computed from the $|J|$'s that may reveal other aspects about the transformations; for example the difference between the signed area of triangles before and after transformation shows volume changes. This is a potential direction for future research. For recent deep learning based registration methods, our digital diffeomorphism criteria has the potential to be used as a loss function to improve the smoothness and promote digitally diffeomorphic transformations.

References

1. IXI Brain Development Dataset. https://brain-development.org/ixi-dataset/
2. Avants, B.B., Epstein, C.L., Grossman, M., Gee, J.C.: Symmetric diffeomorphic image registration with cross-correlation: evaluating automated labeling of elderly and neurodegenerative brain. Medical Image Analysis **12**(1), 26–41 (2008)
3. Balakrishnan, G., Zhao, A., Sabuncu, M.R., Guttag, J., Dalca, A.V.: Voxelmorph: a learning framework for deformable medical image registration. IEEE Transactions on Medical Imaging **38**(8), 1788–1800 (2019)

4. Braden, B.: The surveyor's area formula. The College Mathematics Journal **17**(4), 326–337 (1986)
5. Chen, J., Frey, E.C., He, Y., Segars, W.P., Li, Y., Du, Y.: Transmorph: Transformer for unsupervised medical image registration. Medical Image Analysis **82**, 102615 (2022)
6. Chen, J., He, Y., Frey, E., Li, Y., Du, Y.: ViT-V-Net: Vision transformer for unsupervised volumetric medical image registration. In: Medical Imaging with Deep Learning (2021)
7. Christensen, G.E.: Deformable shape models for anatomy. Washington University in St. Louis (1994)
8. Chvátal, V.: A combinatorial theorem in plane geometry. Journal of Combinatorial Theory, Series B **18**(1), 39–41 (1975)
9. Dalca, A.V., Balakrishnan, G., Guttag, J., Sabuncu, M.R.: Unsupervised learning for fast probabilistic diffeomorphic registration. In: International Conference on Medical Image Computing and Computer-Assisted Intervention. pp. 729–738. Springer (2018)
10. Fischl, B.: Freesurfer. Neuroimage **62**(2), 774–781 (2012)
11. Heinrich, M.P., Maier, O., Handels, H.: Multi-modal multi-atlas segmentation using discrete optimisation and self-similarities. VISCERAL Challenge@ ISBI **1390**, 27 (2015)
12. Hering, A., Hansen, L., Mok, T.C., Chung, A., Siebert, H., Häger, S., Lange, A., Kuckertz, S., Heldmann, S., Shao, W., et al.: Learn2reg: comprehensive multi-task medical image registration challenge, dataset and evaluation in the era of deep learning. arXiv preprint arXiv:2112.04489 (2021)
13. Hoopes, A., Hoffmann, M., Fischl, B., Guttag, J., Dalca, A.V.: Hypermorph: Amortized hyperparameter learning for image registration. In: International Conference on Information Processing in Medical Imaging. pp. 3–17. Springer (2021)
14. Johnson, H.J., Christensen, G.E.: Consistent landmark and intensity-based image registration. IEEE Transactions on Medical Imaging **21**(5), 450–461 (2002)
15. Kabus, S., Klinder, T., Murphy, K., Ginneken, B.v., Lorenz, C., Pluim, J.P.: Evaluation of 4D-CT lung registration. In: International Conference on Medical Image Computing and Computer-Assisted Intervention. pp. 747–754. Springer (2009)
16. Kim, B., Kim, D.H., Park, S.H., Kim, J., Lee, J.G., Ye, J.C.: CycleMorph: cycle consistent unsupervised deformable image registration. Medical Image Analysis **71**, 102036 (2021)
17. LaMontagne, P.J., Benzinger, T.L., Morris, J.C., Keefe, S., Hornbeck, R., Xiong, C., Grant, E., Hassenstab, J., Moulder, K., Vlassenko, A.G., et al.: OASIS-3: Longitudinal neuroimaging, clinical, and cognitive dataset for normal aging and Alzheimer disease. MedRxiv (2019)
18. Liu, Y., Zuo, L., Han, S., Xue, Y., Prince, J.L., Carass, A.: Coordinate translator for learning deformable medical image registration. In: International Workshop on Multiscale Multimodal Medical Imaging. pp. 98–109. Springer (2022)
19. Modat, M., Ridgway, G.R., Taylor, Z.A., Lehmann, M., Barnes, J., Hawkes, D.J., Fox, N.C., Ourselin, S.: Fast free-form deformation using graphics processing units. Computer Methods and Programs in Biomedicine **98**(3), 278–284 (2010)
20. O'Rourke, J., et al.: Art gallery theorems and algorithms, vol. 57. Oxford University Press Oxford (1987)
21. Qiu, H., Qin, C., Schuh, A., Hammernik, K., Rueckert, D.: Learning diffeomorphic and modality-invariant registration using b-splines. In: Medical Imaging with Deep Learning (2021)